Accurate masses of very low mass stars

I. Gl 570BC (0.6 $M_\odot$+0.4 $M_\odot$)[*,**]

Thierry Forveille[1], Jean-Luc Beuzit[2,1,3], Xavier Delfosse[1,3,4], Damien Segransan[1], Francoise Beck[1], Michel Mayor[3], Christian Perrier[1], Andrei Tokovinin[5], and Stéphane Udry[3]

[1] Observatoire de Grenoble, 414 rue de la Piscine, Domaine Universitaire de St Martin d'Hères, 38041 Grenoble, France
[2] Canada-France-Hawaii Telescope Corporation, P.O. Box 1597, Kamuela, HI 96743, USA
[3] Observatoire de Genève, 1290 Sauverny, Switzerland
[4] Instituto de Astrofisica de Canarias, 38200 La Laguna (Tenerife), Spain
[5] Sternberg Astronomical Institute, Universitetsky prosp. 13, 119899 Moscow, Russia

Abstract. We present very accurate individual masses (1.2% relative accuracy) for the two components of Gl 570BC, an interferometric and double-lined spectroscopic binary system. They were obtained from new high accuracy radial velocity and angular separation measurements, analysed together with previously published measurements. From those data we determine a much improved orbit through a simultaneous least square fit to the radial velocity, visual, and parallax information. The derived masses and absolute magnitudes generally validate the theoretical and empirical mass-luminosity relations around 0.5 $M_\odot$, but point towards some low level discrepancies at the 0.1 to 0.15 magnitude level. Forthcoming results of this observing program will extend the comparison to much lower masses with similar accuracy.

Key words: stars: binaries: general – stars: binaries: spectroscopic – stars: binaries: visual – stars: low-mass, brown dwarfs

1. Introduction

Fundamental determination of stellar masses from binary orbits is a most classical astrophysical discipline, last comprehensively reviewed by Andersen (1991; 1998). Besides defining a mean mass-luminosity relation, used at many places in astronomy to approximately convert the observable stellar light to the underlying mass (for instance to derive an initial mass function), accurate stellar masses in multiple systems provide what is perhaps the most demanding and fundamental test of stellar evolution theory (e.g. Andersen 1991). Mass, the basic input of evolutionary models, is directly measured and the models must reproduce the effective temperatures and radii (or luminosities) of both components, for a single age and a single chemical composition. Given the strong dependence of all stellar parameters on mass, this discriminating diagnostic however only shows its power for relative mass errors $\leq$1–2%. In practice this has up to now restricted its use to double-lined detached eclipsing binaries. These systems are however relatively rare: only 44 have yielded masses accurate enough to be included in Andersen's (1991) critical compilation, and few have appeared in the literature since then. Tidally induced rotational mixing may in addition affect the evolution of the short period eclipsing systems, perhaps sufficiently that they are not completely representative of isolated stars. More seriously however, detached eclipsing systems poorly fill some interesting areas in the HR diagram.

The lower main sequence is one major region with very few known eclipsing systems, as a result of the strong observational and intrinsic biases against observing eclipses in faint and physically small stars. Only three well detached eclipsing binaries are known with significantly subsolar component masses: YY Gem (M0Ve, 0.6+0.6 $M_\odot$; Bopp 1974; Leung & Schneider 1978), CM Dra (M4Ve, 0.2+0.2 $M_\odot$; Lacy 1977, Metcalfe et al. 1996), and the recently identified GJ 2069A (M3.5Ve, 0.4+0.4 $M_\odot$; Delfosse et al. 1999a). Detailed observational checks of evolutionary models (e.g. Paczynski & Sienkiewicz 1984; Chabrier & Baraffe 1995) have therefore heavily relied on the first two of these systems, even though they are in some respects non-ideal for this purpose: both binaries have two nearly equal mass components, so that the strength of the differential comparison of two stars with different masses but otherwise equal parameters is largely lost. Also, all three are chromospherically very active, due to tidal synchronisation of their rotation with the short or-

---

bital period. As a consequence, they may have untypical colours for their bolometric luminosity.

Angularly resolved spectroscopic binaries provide stellar masses in parts of the HR diagram where eclipsing systems are missing, though to date these systems have not matched the ∼1% accuracy which can be obtained in detached eclipsing systems. For M dwarfs in particular, the best representation to date of the empirical M-L relation (Henry & Mc Carthy 1993, hereafter HMcC; Henry et al. 1999) still has to rely in part on some fairly noisy mass determinations. For several years (Perrier et al. 1992) we have therefore been following up with high angular resolution some low mass spectroscopic systems found with the CORAVEL or ELODIE radial velocity spectrographs. This follow-up initially used one-dimensional (1D) IR speckle, then two-dimensional (2D) IR speckle, and now uses adaptive optics imaging. As a progress report on this program and as an illustration of our methods, we present here much improved parameters for the double-lined interferometric binary Gl 570BC. The ∼1% accuracy for the 2 masses improves by an order of magnitude on our earlier measurements (Mariotti et al. 1990) of this system, and is getting close to what is obtainable for eclipsing systems.

The Gl 570 system comprises the V=5.7 K4V star Gl 570A (also HR 5568, HD 131977, HIP 73184, FK5 1391), and at a projected distance of 25″ the close Gl 570BC pair (also HD 131976, HIP 73182) which is the subject of the present paper. As discussed below, the orbital period of the close pair is fairly short, only 10 months. Thanks to its small distance of only 6 pc it is nonetheless usually well resolved by the diffraction limit of 4m-class telescopes. The separation within Gl 570BC on the other hand always remains less than 0.2″, so that all seeing-limited measurements refer to integrated properties of the close pair. Its integrated magnitude is V=8.09, and its joint spectral type is M1V (Henry et al. 1994; Reid et al. 1995). The three components have common parallax, proper motion, and radial velocity. They are therefore gravitationnally bound, with the projected separation of the wide pair (about 120 AU at the distance of the system) corresponding to P ∼ 500 years. Formation of the system could either result from the fragmentation of a single gas clump or have involved some capture(s). The latter process however only remains efficient at the high densities which characterize very rich star forming clusters, whose lifetimes are very much shorter than the hydrogen burning timescale in a K4 dwarf. For all practical purposes, the three stars can thus in both cases be considered as coeval and as formed from the same gas.

2. Observations and results

2.1. Angular separation measurements

A variety of astrometric observations of different kinds and of different quality have been collected for Gliese 570BC over the years. The close pair was first resolved by Mariotti et al. (1990) who obtained infrared 1D speckle observations on three occasions and derived a first visual orbit. We refer to their paper for the description of the instrument and the observing and data reduction procedures. HMcC later measured Gl 570BC once with

Table 1. Angular separation measurements

Date	Pos. Angle degree	Separation arc second	Ref.
46961	0	-0.060±0.010	1
46961	90	-0.090±0.010	1
46961	45	-0.110±0.010	1
46961	135	-0.020±0.040	1
47071	0	-0.154±0.025	1
47071	90	-0.097±0.025	1
47274	0	-0.075±0.020	1
47274	45	-0.114±0.010	1
47274	90	-0.094±0.020	1
47343	0	-0.130±0.010	1
47343	45	-0.173±0.010	1
47343	90	-0.114±0.020	1

Date	ρ (arcsec)	θ (degree)	Ref.
47934	0.153±0.006	220.0±2.0	2
48312	0.194±0.010	210.2±3.0	3
48372	0.146±0.020	203.0±5.0	4
49470	0.159±0.004	222.4±1.0	5
49798	0.168±0.004	214.7±2.0	6
50499	0.193±0.002	206.5±0.2	7
50810	0.181±0.004	205.9±0.8	7
51017	0.142±0.005	221.0±2.0	7
51017	0.147±0.006	223.0±2.0	7

Notes: Observation dates are listed as offsets relative to Julian Day 2400000.

References: 1) Mariotti et al. 1990; 2) Henry & Mc Carthy 1993; 3) This paper, Kitt Peak, 2D speckle imager; 4) This paper, ESO 3.6m, COME-ON adaptive optics system; 5) CFHT, CIRCUS 2D speckle imager; 6) ESO 3.6m, ADONIS adaptive optics system; 7) This paper, CFHT, PUE'O adaptive optics system.

a 2D infrared speckle instrument. For readers' convenience, we list these published measurements in Table 1 together with our new 2D speckle and adaptive optics (hereafter AO) observations.

Two measurements were obtained in February 1991 and April 1991 using the speckle mode of the 2D infrared imagers then installed respectively at the KPNO 4.2m telescope and the CFHT 3.6m telescope. Each imager was designed to permit acquisition of exposures short enough to substantially freeze the seeing under standard atmospheric conditions ($t_{exp} \approx 50$ to 100 ms) in bands H and K, independently of the overhead due to read-out time and data transfer time. Several sequences of a few hundred such short exposures were obtained, alternating every few minutes between the source and a nearby unresolved star (usually Gl 570A) used as a point spread function (PSF) calibrator. The whole observation took one hour or less.

In principle, this observing procedure allows an almost simultaneous PSF calibration, and consequently estimates the visibility modulus with 1 to 5% accuracy. We used a software package written specifically for this type of data reduction by E. Tessier (Tessier et al. 1994). It produces an unbiased visibility estimator for the source and then extracts the binary parameters and their estimated variance from this visibility. The actual

detector scale and position angle (P.A.) origin for those observations were calibrated from observations of the astrometric binary ζ Aqr (Heintz 1989).

Most of the new measurements were obtained at the 3.6m Canada-France-Hawaii Telescope (CFHT) on top Mauna Kea, using the CFHT Adaptive Optics Bonnette (Arsenault et al. 1994, Rigaut et al. 1998) and two different infrared cameras (Nadeau et al. 1994, Doyon et al. 1998). Delfosse et al. (1999b) provide a detailed description of the observing procedure, which we therefore don't repeat here. Two observations were also obtained with the ESO 3.6m telescope (La Silla, Chile) AO system COME-ON+ (Rousset & Beuzit 1999), then ADONIS (Beuzit et al. 1997), equipped with the SHARP-II infrared camera, using a similar observing procedure. This COME-ON+ observation has been published in Mariotti et al. (1991). For recent CFHT measurements the corrected point spread function obtained from the AO system was synthesized from simultaneous recordings of the wavefront sensor measurements and deformable mirror commands, as described by Véran et al. (1997). For pre-1997 measurements it was instead obtained from observations of a reference single star of similar R-band magnitude. Astrometric calibration fields such as the central region of the Trapezium Cluster in the Orion Nebula (McCaughrean & Stauffer 1994), were observed to accurately determine the actual detector plate scale and position angle (P.A.) origin. Uncertainties on these parameters do not apreciably contribute to the overall separation error for the small separations in the Gl 570BC system.

The separation, position angle and magnitude difference between the two stars were determined using *uv* plane model fitting in the GILDAS (Grenoble Image and Line Data Analysis System) software, as well as with the deconvolution algorithm described by Véran et al. (1999), coded within IDL. With approximate initial values of the positions of the two components along with the PSF reference image, the fitting procedures gave as output the flux and pixel coordinates of the primary and secondary. Application of the astrometric calibrations then yields the desired parameters.

2.2. Radial velocity measurements

All radial velocity measurements are listed in Table 2 (available in electronic form only). Most of them were obtained with the two CORAVEL radial velocity scanners (Baranne et al. 1979) on the Swiss 1m telescope at Observatoire de Haute Provence (France) and on the Danish 1.54m telescope at La Silla (Chile). The earlier data were previously published by Duquennoy & Mayor (1988) and the system has been regularly observed since then. Gl 570BC is relatively bright for the CORAVEL instruments (V=8.09, Leggett 1992), but both stars are poor matches to the fixed K0III correlation mask. They therefore only produce shallow correlation dips (of which examples were displayed in Duquennoy & Mayor (1988)) and their velocities are measured with typical precisions of respectively 0.7 and 4 km s^{-1}, instead of the usual CORAVEL precision of 0.3 km s^{-1}. The measurements of the M3V secondary in particular were at the limit of the CORAVEL capabilities. During the orbit adjustment discussed
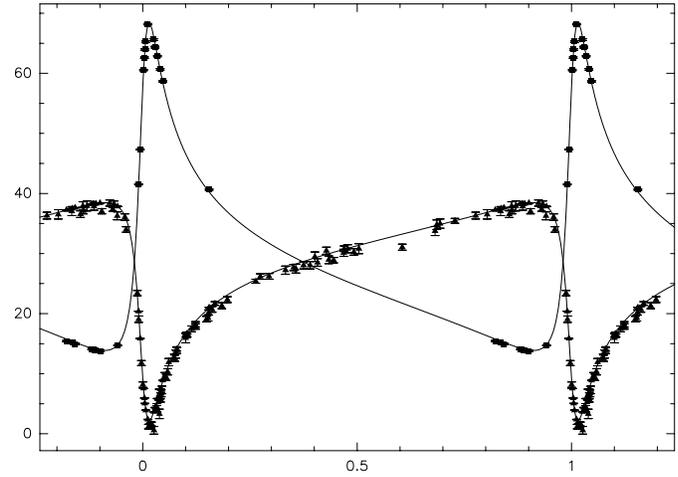

Fig. 1. Radial velocity orbit of the Gl 570BC system. Filled triangles represent measurements of the primary star, and filled squares measurements of the secundary stars. The ELODIE mesurements can be distinguished from the CORAVEL ones by their much smaller error bars.

below they were found to have sizeable systematic errors at phases where the two profiles are even slightly blended. This didn't measurably affect the derived orbital elements since these noisier measurements carried essentially no weight anyway, but they were nonetheless ignored in the final solution. For clarity, they are also not plotted in Fig. 1.

Over the last three years, we have obtained considerably more accurate measurements with the ELODIE spectrograph (Baranne et al. 1996) on the 1.93m telescope of Observatoire de Haute Provence and the CORALIE (Queloz et al. in preparation) spectrograph on the Swiss 1.2m Euler telescope at La Silla (Chile). These echelle spectra were analysed by numerical cross-correlation with an M4V one-bit (i.e. 0/1) mask, as described by Delfosse et al. (1999b). Radial velocities were initially determined by adjusting double gaussians to the correlation profiles. Those however had systematic phase-dependent residuals during the orbital adjustment, which were particularly large (400 m s^{-1} rms) for the fainter secondary star. Upon analysis, they were found to originate from the low level wiggles in the correlation profile of the primary: while the core of this profile is well described by a gaussian function, its baseline doesn't drop to zero as a gaussian would, but instead keeps oscillating at the $\pm 0.2\%$ level, about one tenth of the depth (2%) of the secondary star's dip. Depending on its position on this oscillating background, the measured velocity of the fainter star could therefore be incorrect by up to 1 km s^{-1}. Similar errors of course also affected the measured velocities of the primary star, but they were smaller by the square of the relative depths of the two correlation dips, or a factor of 16. Thanks in part to the excellent stability of the spectrograph, the shape of the correlation profile for a given star is very stable. We could therefore obtain an excellent estimate of the wings of the intrinsic correlation profile of each star, by averaging all profiles of the system, after aligning them at the measured velocity of the star

and blanking all pixels within two profile widths of the velocity of the other star. The residuals of a gaussian adjustment to these average profiles are then subtracted from all correlation profiles, at the measured velocity of each star. This decreases the fluctuation level in the profile baseline to a level of $\pm 0.05\%$. The radial velocities measured by a double gaussian fit to these corrected profiles have typical accuracies of 40 m s^{-1} for the primary and 100 m s^{-1} for the fainter secondary. These residuals are twice larger than would be measured for single-lined spectra with equivalent S/N ratios and correlation dip parameters, but show no systematic phase dependency. They should thus cause no systematic errors on measured parameters.

3. Orbit adjustment

3.1. The adjustment code

The program used for the orbit adjustment, ORBIT, derives from the code of Tokovinin (1992). Like its progenitor, it performs a least square adjustment to all available spectroscopic and "visual" observations, with weights inversely proportional to the square of their standard errors. Besides a number of cosmetic changes, the modifications and additions to Tokovinin (1992) include allowance for multiple radial velocity zero-points, the use of the more robust Levenberg-Marquardt minimisation algorithm, as well as direct support for triple systems. Standard errors for derived parameters (masses, parallax, etc) are computed from the full covariance matrix of the linearized least square adjustment, rather than from just the standard errors of the orbital elements (i.e. the diagonal terms of the covariance matrix). In addition ORBIT can estimate confidence intervals for both derived parameters and orbital elements through Monte-Carlo experiments. For well constrained binaries (like Gl 570BC) these intervals are consistent with the analytic standard errors and gaussian statistics, incidentally providing a check against gross errors in the analytic gradients. For noisier systems though, the vicinity of the minimum of the χ^2 surface becomes significantly non-quadratic. The error statistics for the parameters are then substantially non-gaussian and asymetric, and the Monte-Carlo confidence intervals become an essential feature.

ORBIT also accepts some additional data types, beyond spectroscopic velocities and "visual" (ρ, θ) or (X,Y) pairs. These additions, all of which are used in the present paper, include:

- 1D projected separation measurements, produced by early IR scanning speckle observations and lunar occultations;
- parallaxes, which can be seen as an additional link between the velocity amplitudes, the eccentricity, the period and the semi-major axis; they enter in the least square adjustment with their standard error, providing an optimal unified description between orbital parallaxes of SB2+visual pairs and mass ratios from SB1+visual pairs with a known parallax;
- cross-correlation "dips", produced by correlation velocimeters and cross-correlation analysis of echelle spectra; to support these profiles ORBIT complements the usual list of 10 orbital elements by the width and the equivalent width of

one gaussian profile for each spectroscopic component, and adjusts the 10 orbital elements and the profile parameters directly to the ensemble of all cross-correlations, rho-theta pairs, parallaxes, etc. In a similar manner, modern analyses of long baseline interferometric data sometimes adjust orbital elements (together with magnitude differences) directly to the uv data, avoiding the intermediate step of ρ, θ extraction (Hummel & Amstrong 1992), as do adjustments of visual orbits to Hipparcos Transit Data (Quist & Lindegren 1999; Söderhjelm 1999). A practical inconvenient of this bypassing of intermediate steps is that no individual radial velocities (or ρ, θ, or separations on great circles) are available for compact publication, and that the usual figures of radial velocity curve (or visual orbit) loose sense and become illustrative only. On the positive side however, direct orbital adjustment to the profiles greatly decreases the effective number of degrees of freedom, compared with orbital adjustment to velocities measured from individual profiles. We found that this often improves the error bars on the spectroscopic orbital elements by a factor of two, or better. Global adjustment also considerably reduces the susceptibility of the orbital solution to "pulling" of the velocity of the weaker component towards and away from that of its brighter companion for profiles which are only imperfectly gaussian. In addition, and to further diminish this sensitivity, we produce an average recentered profile for each component, determine residuals to the best fitting gaussian, and subtract those residuals from the individual measurements to then determine iteratively improved parameters.

ORBIT runs on Unix systems and can be obtained from the authors upon request.

To illustrate our methods and the power of combining different data types for the same binary, as probably first advocated by Morbey (1975), we present 3 distinct orbits for Gl 570BC, incorporating successively more of the information available to us. The speckle and adaptive optics data alone turn out to be insufficient to properly define a visual orbit, largely because they never resolve this eccentric system close to its periastron (Fig. 2), where the minimal separation is only $\sim$12 milliarcsecond. As a consequence these data alone leave indeterminate a combination of inclination and semi-major axis with eccentricity. The most restrictive orbit we can present in Table 3 is therefore a spectroscopic one. We then present a combined spectroscopic and visual orbit, and finally an orbit which in addition uses the independent trigonometric parallax of the Gl 570 system.

The longitude of the periastron is given with the spectroscopic convention, and thus refers to the primary. 180° must be added to ω to obtain the visual convention. Table 1 lists the individual speckle and adaptive optics measurements and Table 2 (only available electronically) gives the same information for the radial velocities. Note, though, that the final orbit was directly adjusted to the individual cross-correlation profiles, while the velocities given in Table 2 were determined separately by adjusting two Gaussian curves to each profile. These velocities are
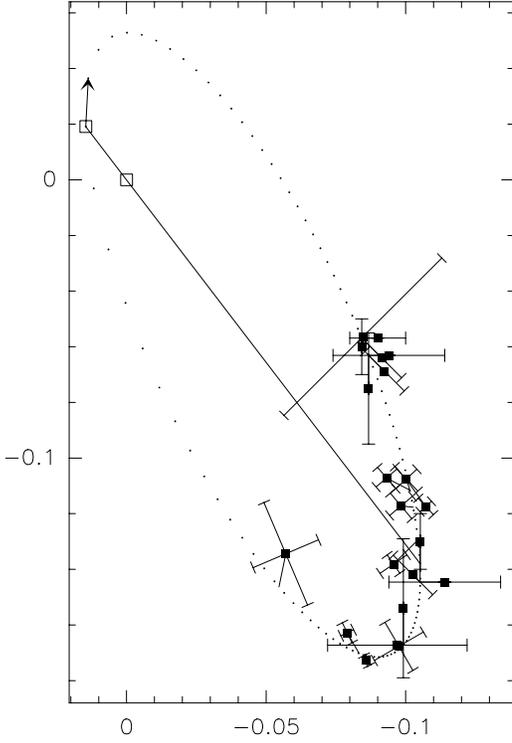
Fig. 2. Visual orbit of the Gl 570BC system. Separations are in arc seconds, North is up and East is left.

Table 3. Orbital elements and derived parameters

Element	Spectro	Spectro+OA	Spectro+OA+π
V_0 (km s^{-1})	28.664±0.008	28.665±0.008	28.665±0.008
P (days)	308.884±0.004	308.884±0.004	308.884±0.004
T_0 (JD)	270.220±0.011	270.220±0.011	270.220±0.011
e	0.7559±0.0002	0.7559±0.0002	0.7559±0.0002
a (arcsec)	–	0.1514±0.0015	0.1507±0.0007
Ω_1 (deg)	–	196.2±0.7	195.9±0.5
ω_1 (deg)	127.56±0.05	127.56±0.05	127.56±0.05
i (deg)	–	107.2±1.0	107.6±0.7
K_1 (km s^{-1})	18.187±0.008	18.187±0.008	18.187±0.008
K_2 (km s^{-1})	27.325±0.026	27.324±0.026	27.325±0.026
W_1 (km s^{-1})	6.169±0.008	6.169±0.008	6.169±0.008
W_2 (km s^{-1})	5.643±0.030	5.642±0.030	5.642±0.030
EW_1 (km s^{-1})	0.4532±0.0005	0.4532±0.0005	0.4532±0.0005
EW_2 (km s^{-1})	0.1041±0.0005	0.1041±0.0005	0.1041±0.0005
$\Delta V_{CRV-ELO}$	-0.633±0.065	-0.633±0.065	-0.633±0.065
Derived parameters:			
$M_1 \times sin^3 i$ ($M_\odot$)	0.5082±0.0011	0.5082±0.0011	0.5083±0.0011
$M_2 \times sin^3 i$ ($M_\odot$)	0.3383±0.0005	0.3383±0.0005	0.3383±0.0005
M_1 ($M_\odot$)	–	0.583±0.009	0.586±0.007
M_2 ($M_\odot$)	–	0.388±0.006	0.390±0.005
π (arcsec)	–	0.1710±0.0022	0.1698±0.0009

Notes: Epochs are listed as offsets relative to Julian Day 2450000. W_1 and W_2 are the full widths to half power of the Gaussian function for the two components, while EW_1 and and EW_2 are their equivalent widths. The other orbital elements have their usual meaning.

given here mostly for illustrative purposes, as plotted in Fig. 1. Their use would give a slightly different (and noisier) solution, but may nonetheless prove convenient. There is no compact way to publish the full information needed to reproduce our analysis, since it does not proceed through determining radial velocities as an intermediate step. We will make the digital correlation profiles available upon request to the first author. Fig. 2 shows the visual data and orbit.

3.2. Spectroscopic orbit

As mentioned above, the spectroscopic orbit presented in Table 3 was adjusted directly to the correlation profiles rather than to the extracted radial velocities. As can be seen, the spectroscopic quantities $M \times sin^3 i$ are determined with very high accuracies of 0.2%. The relatively few ELODIE measurements contribute considerably to the overall precision of the orbital solution, and ignoring them would for instance degrade the standard errors of the $M \times sin^3 i$ by an order of magnitude. The much more numerous CORAVEL measurements of the primary star by contrast only contribute to an improved orbital period, thanks to their much longer timespan. They otherwise carry very little weight in the solution.

3.3. Spectroscopic+visual orbit

Inclusion of the speckle and adaptive optics data in the adjustment leaves all spectroscopic elements essentially unchanged (Table 3), but determines the three otherwise unknown orbital

elements: the semi-major axis (a), the inclination (i), and the orientation of the projected orbit on the sky (Ω). Individual stellar masses as well as an orbital parallax for the system can then be derived from the full complement of orbital elements, and are also listed in Table 3. The standard errors computed from the covariance matrix were checked through Monte-Carlo simulations, which resulted in confidence intervals that were fully consistent with gaussian errors of the stated dispersion. This verifies that non-linearities in the least square adjustment are negligible for this very well constrained system. The two masses are determined here with 1.6% accuracy, and the orbital parallax to within 2.2 milliarcsecond (1.3%).

The availability of Hipparcos parallaxes represents an opportunity to independently verify the orbital parallax, and thus to globally check the orbital solution for systematic errors. Though somewhat noisier than typical for a V=5.7 star, the Hipparcos catalog parallax of Gl 570A is well determined, π=0.1693±0.0018″. The parallax for Gl 570BC itself has very large error bars ($\sigma(\pi)$=0.033″) in the Hipparcos catalog (ESA 1997), because the unaccounted orbital motion with P$\sim$0.8 year strongly couples into the parallax solution over the limited lifetime of the Hipparcos satellite. Fortunately, Söderhjelm (1999) recently reanalysed the Hipparcos intermediate transit data, accounting for the orbital motion within Gl 570BC, and obtained sharply reduced error bars for the trigonometric parallax: π=0.1697″±0.0010″. The two astrometric determinations are mutually consistent and agree with the orbital parallax of 0.1710±0.0022″, to within better than 1 σ.

3.4. Spectroscopic+Visual+Parallax orbit

Instead of using the independent trigonometric parallaxes as a sanity check for the orbital solution, ORBIT offers the option to consider it as an additional observation, linking i, e, P, a and K_1+K_2. It is then included in the combined least square adjustment, together with the radial velocities and angular separations. This very significantly improves the determinacy of the least square system, and in particular reduces the standard errors of the semi-major axis by a factor of 2. We note here that it would be preferable, at least conceptually, to adjust an orbit directly to the Hipparcos transit data rather than to the Hipparcos parallax. ORBIT does not yet support this data type however, which we plan to add in the near future.

The contributions to the overall χ^2 of the different data types included in the solution are approximately consistent with their respective number of measurements. This indicates that there are no large systematic errors in any one data type, and that the adopted standard errors are at least approximately correct. This orbit (last column of Table 3) has the smallest errorbars (and smallest covariances) for all orbital elements. It is consistent with all previously published orbits to within their stated error bars, after allowing for the 180° ambiguity in the identification of the ascending node (i.e. Ω) in purely visual orbits. We adopt it as our preferred solution for the rest of the discussion. The inclusion of the trigonometric parallax information improves the relative accuracy of the two masses to 1.2%: $M_1 = 0.586 \pm 0.007\, M_\odot$ and $M_2 = 0.390 \pm 0.005\, M_\odot$. They are consistent with the values obtained by Mariotti et al. (1990) to within a fraction of their quoted standard deviation, as well as with the mass sum derived by Söderhjelm (1999) from an analysis of the Hipparcos transit data, but improve on their accuracy by over a factor of 5. These accuracies are among the best obtained to date for non-eclipsing binaries, but still do not match the $\sim 0.2\%$ obtained for the spectroscopic $M \times sin^3 i$. There is thus still room for improvement in the astrometric measurements. We are conducting some long baseline interferometric observations of Gl 570BC (Segransan et al. in progress) with IOTA (Millan-Gabet et al. 1999), which have the potential to ultimately match the sub-% spectroscopic accuracy for the masses. The "resulting" parallax in the last column of Table 3), $0.1698 \pm 0.0009''$, is computed as an orbital parallax from the elements of this combined orbit, which themselves take the trigonometric parallax into account. It is an optimal combination of the distance information available in the trigonometric parallax and in the orbit. In the present case is mostly determined by the weighted average of the two HIPPARCOS parallaxes, with little contribution from the orbit.

4. Luminosities and colours

Photometric measurements of the combined light of the system have been made by a number of authors over a broad range of colours. They are summarised and homogenized in the critical compilation of Leggett (1992), from which we adopt: U=10.79, B=9.57,V=8.09, R=7.09, I=5.97, J=4.75, H=4.14, K=3.93, L=3.77, L'=3.67, with quoted errors of <3% on IJHK. The system has colours consistent with those of solar metal-

Table 4. Absolute magnitudes of the two components

	Primary	Secondary
M_J	6.213±0.033	7.403 ±0.039
M_H	5.613±0.033	6.763 ±0.039
M_K	5.396±0.033	6.576 ±0.039
M_L	5.167±0.111	6.227 ±0.159

licity stars (Leggett 1992), as expected from the spectroscopic metallicity discussed below.

The difference in brightness between the components of Gl 570BC has been measured on several occasions in different bandpasses. Mariotti et al. (1990) obtained magnitude differences of Δ_J=1.27±0.12, Δ_H=1.19±0.12, Δ_K=1.12±0.07, and Δ'_L=1.06±0.17 from their 1D scanning speckle observations. HMcC published another estimate in the J band, Δ_J=1.30±0.04. Our own adaptive optics measurements provide Δ_K=1.18±0.04, as well as Δ_m=1.18±0.04 in a narrow band Br_γ (2.166μm) filter. We estimate a correction of $\Delta_K - \Delta_{Br_\gamma}$=0.04, using synthetic photometry generated from NextGen (Hauschild, Allard, & Baron 1999) model spectra of effective temperatures that bracket those apropriate for M dwarfs of the luminosities of the two components of Gl 570BC. This provides a second determination of the K band flux ratio, Δ_K=1.22±0.04.

While those measurements are mutually consistent for every filter, their run with wavelenghth is only marginally compatible with the known IR colours of M dwarfs (Leggett 1992). The $J - H$ and (particularly) $J - K$ colours of early and mid-M dwarfs define a remarkably flat plateau (Leggett 1992): when the spectral type of solar metallicity stars (apropriate for Gl 570BC) varies between M0V ($M_K \sim 4.8$) and M5.5V ($M_K \sim 7.9$), $J-H$ only changes from 0.68 to 0.57, and $J-K$ just from 0.85 to 0.87 (Leggett 1992) The two components of Gl 570BC respectively have $M_K \sim 5.4$ and $M_K \sim 6.6$ and their $J-H$ and $J-K$ colours are therefore expected to only differ by about -0.04 and +0.01. Δ_J should therefore be almost identical to Δ_K, whereas the observations give Δ_J-Δ_K=0.14±0.04, and Δ_J-Δ_H should be -0.04, whereas the observations indicate Δ_J-Δ_H=+0.11±0.12. As the integrated colours of the system match the expected values, this inconsistency must come from some of the measured magnitude differences. We suspect that it traces back to an overestimated contrast in the J and H band observations of both Mariotti et al. (1990) and HMcC, since speckle techniques have a known bias towards underestimating the relative flux of faint components (Perrier 1988). The K band adaptive optics observations are in principle immune to this bias, and the K band speckle observations of Mariotti et al. (1990) should be relatively unaffected, thanks to the low D/r_0 (where D is the telescope diameter and r_0 is the Fried parameter of the atmosphere) at this longer wavelength. We therefore tentatively adopt as the basis of our magnitude difference system the mean of the three K band measurements, Δ_K=1.18±0.03. From this value we then derive preferred values of Δ_J=1.19 and Δ_H=1.15, but we will also consider the published J and K flux ratios as an alternative. This discrepancy contributes significant uncertainty

to the analysis, and better measurements of the flux ratios at J and H would be of considerable interest. To date all our adaptive optics measurements in the J and H bands have unfortunately been obtained at phases when the secondary star overlaps the first Airy ring of the primary for these wavelengths. These circumstances maximize the uncertainties in differential photometry from partially corrected adaptive optics images (Veran et al. 1999), and these data therefore contribute no useful information on the flux density ratio.

Absolute magnitudes were derived from the parallax and the apparent magnitudes of the individual stars. The absolute magnitudes of the brighter star have uncertainties which are dominated by those of the photometry of the system, while those for the secondary have some contribution from the magnitude difference. The parallax doesn't appreciably contribute in either case.

5. Discussion and conclusions

The accurate masses and absolute magnitudes that we have obtained for the Gl 570BC system represent a new benchmark for model calculations (e.g. Baraffe et al. 1998) and an independent check of the empirical mass-luminosity relations (HMcC). The constraints which they bring to the models are largely complementary to those coming from the eclipsing binaries, whose absolute radii can be determined very accurately but whose larger distances on the other hand contribute significant uncertainties to the absolute magnitudes.

As long emphasized by theoreticians, and by observers of more massive stars (e.g. Andersen 1991), there is however no such thing as one single mass-luminosity relation: stellar luminosities depend on chemical composition as well as on mass (in general they depend on age too, though not in the age and mass range discussed here). Quantitative metallicity determinations however are notoriously difficult for M dwarfs (e.g. Viti et al. 1997; Valenti et al. 1998). Observers in this field usually have to resort to photometric metallicity estimators (Leggett 1992) which are only approximately calibrated, or otherwise assume by default a solar metallicity. Thanks to its physical association with the hotter Gl 570A (K4V), the Gl 570BC pair represents a rare case of two M dwarfs with a very well determined spectroscopic metallicity. Its accurate masses are thus fortunately matched with excellent metallicities. Hearnshaw (1976) first measured the metallicity of Gl 570A from high resolution electronographic spectra and obtained [Fe/H]=+0.01±0.15. More recently, Feltzing & Gustafsson (1998) measured [Fe/H]=0.04±0.02(random)±0.1(systematic) from high S/N R=10^5 echelle CCD spectra. These authors find some evidence for NLTE overionisation of Fe into Fe^+, but the derived elemental Fe abundance is unaffected, as Fe is overwhelmingly neutral in the photosphere of a K4 dwarf. Quite conveniently for comparison with published models, the Gl 570 system thus has a truly solar metallicity.

Fig. 3 compares the mass and luminosity of the two components of Gl 570BC with the Baraffe et al. (1998) 10 Gyr solar-metallicity isochrone. These models consistently combine
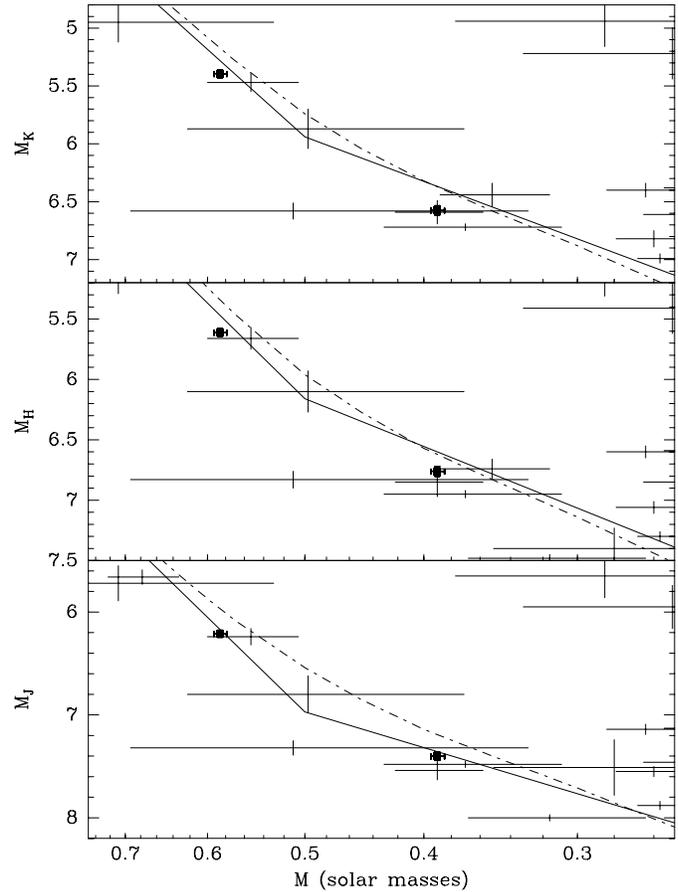

Fig. 3. Near-IR Mass-Luminosity diagrams for mid-M dwarfs. The square symbols with thick error bars correspond to the two components of Gl 570BC, and the thin error-bars represent data from HMcC. The solid and dot-dashed lines respectively represent the empirical HMcC analytical Mass-Luminosity relation and the theoretical [M/H]=0.0 10 Gyr isochrone of Baraffe et al. (1998).

stellar evolution models (e.g. Chabrier & Baraffe 1997) and non-grey atmospheric models (Allard & Hauschild 1995; Hauschild et al. 1999). The present generation of these evolutionary models still uses non-dusty atmospheres, but dust only becomes relevant at effective temperatures significantly lower than those of Gl 570BC (Allard 1998). The Baraffe et al. models are consistently slightly brighter in all 3 bands than the two stars, by 0.08 to 0.15 magnitude. While this level of agreement is already very comforting, the discrepancies are significant at the $\sim 3\sigma$ levels and may point towards remaining low level deficiencies of the theoretical models. If one adopts the measured J and H band flux ratios, rather than the smaller values that we have estimated from the K band measurement, the agreement with the models improves only slightly for the primary star, as its magnitude only weakly depends on the exact value of the large flux ratio. At the same time this choice degrades the agreement for the fainter star by a larger factor, and the overall agreement with the models is significantly worse.

Fig. 3 also shows the data points of HMcC, as well as their analytic representation of those data. The agreement is essen-

tially perfect with the J band HMcC relation, while the H and K band relations are slightly discrepant, by respectively 0.1 and 0.15 magnitudes. We note that the HMcC mass-luminosity relations are only consistent with the empirical M dwarf colours of Leggett (1992) at this 0.10–0.15 magnitude level, even though the HMcC photometry mostly traces back to Leggett (1992). This is because the HMcC mass-magnitude relations for J, H and K were adjusted independently, without explicit forcing of colour consistency. The perfect agreement with the J band HMcC fit is therefore probably fortuitous to some extent, and the 0.10 to 0.15 discrepancy for the H and K bands probably represents a more realistic estimate of the accuracy of those analytic fits around 0.5 $M_\odot$.

References

Allard F., Hauschild P. 1995, ApJ 445, 433.

Allard F. 1998, p. 370 in "Brown dwarfs and extrasolar planets", Rebolo R., Martín E.L., Zapatero Osorio M. R., Eds., ASP Conference Series #134.

Andersen J. 1991, Astronomy and Astrophysics Review 3, 91.

Andersen J. 1998, p. 99 in Fundamental Stellar Properties: The Interaction between Observations and Theory, IAU Colloquium 189, T. R. Bedding et al., Eds., Kluwer: Dordrecht.

Arsenault R., Salmon D., Kerr J., Rigaut F., Cramton D., Grundmann W.A., 1994, in SPIEE Proceedings 2201, "Adaptive Optics in Astronomy", eds. M.A. Ealey, F. Merkle, 833

Baraffe I., Chabrier G., Allard F., Hautschildt P. H., 1998, A&A 337, 403.

Baranne A., Mayor M., Poncet J.L. 1979, Vistas in Astronomy 23, 279.

Baranne A., Queloz D., Mayor M., et al., 1996 A&ASupp. 119, 373.

Beuzit J.-L., Demailly L., Gendron E., et al., 1997, Experimental Astronomy 7, 285

Bopp B.W. 1974, ApJ 193, 389.

Chabrier G. and Baraffe I. 1995, ApJ 451, L21.

Chabrier G. and Baraffe I. 1997, A&A 327, 1039.

Delfosse X., Forveille T., Mayor M., Burnet M., Perrier C., 1999a, A&A 341, L63.

Delfosse X., Forveille T., Beuzit J.L., Udry S., Mayor M. and Perrier C. 1999b, A&A 344, 897.

Doyon R., Nadeau D., Vallée P., et al., 1998, in SPIE Proceedings 3354, "Infrared Astronomical Instrumentation", ed. A.M. Fowler, 760.

Duquennoy A. and Mayor M. 1988, A&A 200, 135.

ESA, 1997, The HIPPARCOS Catalogue, ESA SP-1200

Feltzing S. and Gustafsson B., 1998, A&ASupp. 129, 237.

Hauschild P, Allard F., Baron E., 1999, ApJ 512, 377.

Hearnshaw J.B. 1976, A&A 51, 85.

Heintz, W.D. 1989 A&A 217, 145

Henry T.J., Mc Carthy Jr D.W. 1993, AJ 106, 773 (HMcC).

Henry T.J., Franz O.G., Wasserman L.H., et al., 1999, ApJ 512, 864.

Henry T. J., Kirkpatrick J.D., Simons D. A., 1994, AJ 108, 1437.

Hummel C.A., Armstrong J.T. 1992, in "ESO Conference on High-Resolution Imaging by Interferometry II. Ground-Based Interferometry at Visible and Infrared Wavelengths", J.M. Beckers, F. Merkle Eds, European Southern Observatory, Garching bei Munchen, Germany.

Lacy C.H. 1977, ApJ 218, 444.

Leggett S.K., 1992, ApJSupp. 82, 351

Leung K.C. and Schneider D.P. 1978, AJ 94, 712.

Mariotti J.M., Perrier C., Duquennoy A., Duhoux P. 1990, A&A 230, 77.

Mariotti J.-M., Perrier C., Duquennoy A., et al., 1991, ESO conf. on High-Resolution Imaging by Interferometry. II p99–107.

Mc Caughrean M.J., Stauffer J.R. 1994, AJ 108, 1382.

Metcalfe T.S., Mathieu R.D., Latham D.W. and Torres G. 1996, ApJ 456, 356.

Millan-Gabet R., Schloerb F.P., Traub W.A., Carleton F.P., 1999, PASP 111, 238.

Morbey C.L. 1975, PASP 87, 689.

Nadeau D., Murphy D.C., Doyon R., Rowlands N., 1994, PASP 106, 909

Paczynski B. and Sienkiewicz R. 1984, ApJ 286, 332.

Perrier C. 1988, p. 99. in "High-Resolution Imaging by Interferometry", NATO ASI Series, Kluwer (Dordrecht), edited by D.Alloin and J.M. Mariotti.

Perrier C., Duquennoy A., Mariotti J.M., Mayor M., Morbey C., 1992, p. 543. in "Complementary Approaches to Double and Multiple Star Research", ASP Conference Series, Vol. 32, IAU Colloquium 135, McAlister H.A. and Hartkopf W.I., Eds.

Quist C.F. and Lindegren L., 1999, Astron. Astrophys. Suppl. Ser. 138, 327.

Reid I.N., Hawley S.L., and Gizis J.E., 1995, AJ 110, 1838.

Rigaut F., Salmon D., Arsenault R., et al., 1998, PASP 110, 152.

Rousset G. and Beuzit J.-L., 1999, "The ESO systems", in "Adaptive Optics in Astronomy", F. Roddier Ed., Cambridge University Press

Söderhjelm 1999, A&A 341, 121

Tessier, E., Bouvier, J., Lacombe F. 1994, A&A 283, 827.

Tokovinin A. 1992, in Complementary Approaches to Double and Multiple Stars Research, IAU Colloquium 135, ASP Conf. Series, Vol 32, edited by H.A. Mc Alister and W.I. Hartkopf (ASP, San Francisco), p573.

Valenti J. A., Piskunov N., Johns-Krull C. M., 1998, ApJ 498, 851.

Véran J.-P., Rigaut F., Rouan D., Maitre H., 1997, J. Opt. Soc. Am. A 14(11), 3057

Véran J.P., Beuzit, J.L., Chaytor D. 1999, p. 691 in "ESO/OSA Topical Meeting on Astronomy with Adaptive Optics", ESO Conference Series 56, Edited by D. Bonacini.

Viti S., Jones H.R.A., Schweitzer A., et al., 1997, MNRAS 291, 780.